

Vacuum Energy and Topological Mass in Interacting Elko and Scalar Field Theories

¹A. J. D. Farias Junior , ^{*}²A. Smirnov,  ³Herondy F. Santana Mota ,  and ³E. R. Bezerra de Mello , 

¹*Instituto Federal de Alagoas,
CEP 57466-034, Piranhas, Alagoas, Brazil*
²*Departamento de Física, Universidade Federal de Sergipe,
CEP 49107-230, São Cristóvão, Sergipe, Brazil and*
³*Departamento de Física, Universidade Federal da Paraíba,
Caixa Postal 5008, João Pessoa, Paraíba, Brazil*

In this paper, we consider a four-dimensional system composed of a mass-dimension-one fermionic field, also known as Elko, interacting with a real scalar field. Our main objective is to analyze the Casimir effects associated with this system, assuming that both the Elko and scalar fields satisfy Dirichlet boundary conditions on two large parallel plates separated by a distance L . In this scenario, we calculate the vacuum energy density and its first-order correction in the coupling constants of the theory. Additionally, we consider the mass correction for each field separately, namely the topological mass that arises from the boundary conditions imposed on the fields and which also depends on the coupling constants. To develop this analysis, we use the mathematical formalism known as the effective potential, expressed as a path integral in quantum field theory.

I. INTRODUCTION

One of the most important results in theoretical physics was obtained by H. Casimir in 1948 [1]. Casimir proposed that two large, neutral, conducting, parallel plates are subjected to an attractive force. The theoretical description of this effect lies within the framework of quantum field theory, specifically the quantized electromagnetic field. The boundary conditions imposed on the plates modify the vacuum fluctuations, giving rise to the attractive force between them. The first experimental attempt to detect the Casimir effect was carried out by Sparnaay in 1958 [2], but it failed to accurately confirm the phenomenon due to insufficient precision. Several decades later, the Casimir effect was successfully observed and measured in a series of high-accuracy experiments, both for parallel plates [3] and for other geometries [4–9]. From a theoretical perspective, it has been generalized to different quantum fields, geometries, boundary conditions, and even curved spacetimes, becoming a valuable tool for probing fundamental aspects of quantum field theory and for potential applications in nanotechnology, condensed matter systems, and cosmology [10–15]. Comprehensive reviews of the Casimir effect and its generalizations can be found in Refs. [11, 16, 17].

Beyond the electromagnetic case, it is now well established that scalar and fermionic fields also develop Casimir-like effects. Scalar fields under Robin or helix boundary conditions, or in noncommutative backgrounds, display rich vacuum structures and thermal corrections [18–20]. Fermionic fields, on the other hand, present additional subtleties related to their anticommuting nature and boundary conditions, as in the MIT bag model or in spacetimes with nontrivial topology [21–23]. Among these, an especially interesting case is the so-called Elko field, a fermionic quantum field with mass dimension one. In this scenario, the Casimir effect was considered in Refs. [24, 25].

Elko fields were first introduced by Ahluwalia and Grumiller [26] as eigenspinors of the charge conjugation operator. Unlike Dirac and Majorana spinors, Elko spinors belong to a non-standard Wigner class of representations, possessing unusual transformation properties under the Lorentz group. In particular, they transform under a non-local representation of Lorentz symmetry, which preserves locality only along a preferred axis. This peculiar structure forces the Elko field to have canonical mass dimension one, rather than the usual 3/2 for fermions, which drastically restricts the types of renormalizable interactions it may admit. In fact, the Elko field can only couple renormalizably to scalar degrees of freedom, most notably the Higgs field, and possibly to gravity. These features render it largely invisible to Standard Model gauge interactions, making Elko a natural dark matter candidate.

^{*} antonio.farias@ifal.edu.br

[†] smirnov@ufs.br

[‡] hmota@fisica.ufpb.br

[§] emello@fisica.ufpb.br

From the perspective of high-energy physics and cosmology, Elko fields have been extensively discussed as components of dark matter models, due to their suppressed couplings to ordinary matter and gauge bosons. They have also been considered in inflationary scenarios, as drivers of accelerated expansion, and in models of late-time cosmic acceleration where Elko condensates mimic dark energy. These applications highlight their versatility and justify the study of Elko in diverse quantum and cosmological settings [24–27]. In particular, Casimir-like effects associated with Elko fields offer a way to explore how exotic spinors interact with boundaries and topology [24, 25], thereby linking fundamental field-theoretical properties with potentially observable macroscopic phenomena.

A natural step forward is to investigate Elko fields in interaction with scalar fields. From the viewpoint of renormalizable Quantum Field Theory (QFT), this is the most viable scenario, since Elko can couple quadratically to a scalar field through a dimensionless coupling constant. In the context of particle physics, such an interaction resonates with the Higgs mechanism, suggesting possible consequences for mass generation and for dark matter phenomenology. From the perspective of effective field theory, including both a quadratic Elko-scalar coupling and a quartic scalar self-interaction is the minimal and consistent extension to study nontrivial quantum corrections such as loop effects and induced topological masses.

In order to capture boundary effects, we impose Dirichlet boundary conditions on both the Elko and the real scalar field. Physically, this corresponds to confining the fields between two parallel, perfectly reflecting plates separated by a distance L . Such conditions fix the allowed mode spectrum, directly modifying the vacuum fluctuations and thereby shaping the vacuum energy. Dirichlet boundary conditions are particularly well-suited for analytical progress, and they provide a natural comparison with the electromagnetic Casimir effect in idealized geometries. Moreover, by enforcing the same boundary conditions on both fields, we ensure a consistent framework to analyze interaction effects in the vacuum energy and in the generation of topological masses.

In this work, we analyze a four-dimensional system composed of an Elko fermionic field interacting with a real scalar field through a quadratic coupling, while also including a quartic self-interaction for the scalar sector. Both fields are subjected to Dirichlet boundary conditions on two large, parallel plates separated by a distance L . Employing the path integral formalism and the effective potential method [28], we compute the vacuum energy density (Casimir-like effect), its first-order interaction corrections, and the topological masses induced in each field by the combined effect of interactions and boundary conditions. In particular, we show that the Elko contribution to the vacuum energy is enhanced relative to the scalar case, and that first-order coupling corrections give rise to nontrivial boundary-induced mass shifts. These results extend previous analyses of non-interacting fields [24, 25] and highlight how exotic fermions with suppressed Standard Model interactions can nonetheless manifest observable quantum vacuum effects.

It is worth mentioning that in the scalar sector the topological mass correction may turn negative, which signals the possibility of vacuum instability or symmetry breaking induced by the boundaries. In such situations, a more refined vacuum stability analysis would be required in order to determine consistent and physically acceptable values for the effective scalar mass. This type of analysis naturally connects with the existence of other possible vacua of the theory, and may reveal boundary-driven phase transitions between distinct vacuum configurations.

Finally, we note that the effective potential in the present model depends simultaneously on three background variables, associated with the Elko field bilinear, the scalar field, and their mutual interaction. This richer structure increases the possibility of multiple competing vacua, which may correspond to distinct phases of the theory. While a detailed exploration of such a vacuum landscape is beyond the scope of the present work, its existence could have important implications: in some regimes the true ground state may differ from the perturbative one, or metastable vacua may arise, potentially leading to boundary-induced phase transitions. Understanding whether these additional minima carry physical consequences, or are merely artifacts of the approximation scheme, requires a systematic vacuum stability analysis, which we leave for future investigation.

The structure of the paper is as follows. In Sec. II we introduce the model, define the interacting Lagrangian, and set up the effective potential. In Sec. III we compute the one-loop corrections using the generalized zeta-function regularization. Sec. IV is devoted to the evaluation of the vacuum energy per unit area of the plates, including first-order coupling-constant corrections and the emergence of topological masses. Finally, in Sec. V we present our concluding remarks and perspectives for future work.

Through this paper we use natural units in which both the Planck constant and the speed of light are set equal to one, $\hbar = c = 1$.

II. EFFECTIVE POTENTIAL OF THE ELKO FIELD INTERACTING WITH A REAL SCALAR FIELD

We consider a system composed of a spin-1/2 fermionic field with mass dimension one, known as the Elko field, interacting (for simplicity) with a real scalar field. The Euclidean action of the Elko field, including also a Elko-scalar field interaction, is given by [27]:

$$S(\bar{\eta}, \eta, \varphi) = S_E + S_R + S_{\text{int}}, \quad (1)$$

where S_E denotes the action of the free Elko field,

$$S_E(\bar{\eta}, \eta) = - \int d^4x (-\bar{\eta} \square \eta + m_E^2 \bar{\eta} \eta), \quad \square = \partial_t^2 + \nabla^2. \quad (2)$$

Here, η represents the Elko field, $\bar{\eta}$ its conjugate, and m_E is its mass.

The term S_R corresponds to the action of the scalar field, including the quartic self-interaction:

$$S_R(\varphi) = -\frac{1}{2} \int d^4x (-\varphi \square \varphi + m_R^2 \varphi^2) - \int d^4x \frac{\lambda_\varphi}{4!} \varphi^4, \quad (3)$$

where φ represents the real scalar field, m_R its mass, and λ_φ the quartic self-coupling constant.

Finally, the Elko-scalar field interaction action is defined as [27]:

$$S_{\text{int}}(\bar{\eta}, \eta, \varphi) = - \int d^4x g \varphi^2 \bar{\eta} \eta, \quad (4)$$

where g is the coupling constant characterizing the interaction between the Elko and scalar fields.

For the system described above, the vacuum-to-vacuum transition function is written as

$$Z(\bar{\eta}, \eta, \varphi) = \int \mathcal{D}\bar{\eta} \mathcal{D}\eta \mathcal{D}\varphi \exp(S_E + S_R + S_{\text{int}}). \quad (5)$$

In order to construct the effective potential, we use the path integral approach. In this paper, we follow the procedure detailed in Refs. [28–30] (see also [31–33]). For the reader’s convenience, we present only the main steps.

We shift the fields around fixed background fields, i.e.,

$$\eta = \Psi + \chi, \quad \varphi = \Phi + \rho, \quad (6)$$

where χ and ρ represent quantum fluctuations, and Ψ and Φ are fixed classical background fields. Note that Φ is a scalar field, while Ψ is a single Grassmann variable, reflecting the fermionic nature of the Elko field. The procedure above is analogous to what was done in Ref. [33]. In contrast, in the present case, due to the fermionic nature of the Elko field, there is no need to set $\Phi = 0$ in advance, unlike in [33].

The effective potential can then be expanded as

$$V_{\text{eff}}(\bar{\Psi}, \Psi, \Phi) = V^{(0)}(\bar{\Psi}, \Psi, \Phi) + V^{(1)}(\bar{\Psi}, \Psi, \Phi) + V^{(2)}(\bar{\Psi}, \Psi, \Phi), \quad (7)$$

where $V^{(0)}$ is the classical (tree-level) contribution:

$$V^{(0)}(\bar{\Psi}, \Psi, \Phi) = m_E^2 \bar{\Psi} \Psi + m_R^2 \Phi^2 + \frac{\lambda_\varphi}{4!} \Phi^4 + g \Phi^2 \bar{\Psi} \Psi + \xi(\bar{\Psi}, \Psi, \Phi, C_i), \quad (8)$$

with

$$\xi(\bar{\Psi}, \Psi, \Phi, C_i) = \frac{C_1}{4!} \Phi^4 + \frac{C_2}{2} \Phi^2 + C_3 + C_4 \bar{\Psi} \Psi + C_5 \Phi^2 \bar{\Psi} \Psi, \quad (9)$$

representing the renormalization contributions with constants C_i ($i = 1, \dots, 5$).

The one-loop contribution $V^{(1)}$ can be expressed as a path integral [33, 34], that is,

$$V^{(1)}(\bar{\Psi}, \Psi, \Phi) = -\frac{1}{\Omega_4} \ln \int \mathcal{D}\bar{\eta} \mathcal{D}\eta \mathcal{D}\varphi \exp \left[- \int d^4x \bar{\eta} \hat{A} \eta - \frac{1}{2} \int d^4x \varphi \hat{B} \varphi \right], \quad (10)$$

where Ω_4 is the four-dimensional spacetime volume and the operators \hat{A} and \hat{B} are defined as

$$\begin{aligned}\hat{A} &= (-\square + m_E^2 + g\Phi^2) \mathbf{1}_{4 \times 4}, \\ \hat{B} &= -\square + m_R^2 + \frac{\lambda_\varphi}{2}\Phi^2 + 2g\bar{\Psi}\Psi,\end{aligned}\quad (11)$$

with $\mathbf{1}_{4 \times 4}$ denoting the 4×4 identity matrix.

The two-loop contribution $V^{(2)}$ is most conveniently computed using the Feynman diagrams of the theory under consideration, which will be done in Sec. IV.

Given the form of the one-loop correction in Eq. (10), we can separate the contributions from each field in the path integral. The path integral associated with the real scalar field has been written in a convenient form in several references [32–34]. Now, for the Elko field we write

$$V_E^{(1)} = -\frac{1}{\Omega_4} \ln \int \mathcal{D}\bar{\eta} \mathcal{D}\eta \exp \left(-\int d^4x \bar{\eta} \hat{A} \eta \right). \quad (12)$$

To write $V_E^{(1)}$ we follow the steps described in [35], although some of these steps are indicated here. First, we assume that the operator \hat{A} has a complete set of eigenfunctions and eigenvalues, i.e.,

$$\hat{A}\psi_j = \Lambda_j \psi_j, \quad \int d^4x \psi_i^\dagger(x) \psi_j(x) = \delta_{ij}. \quad (13)$$

Since $\{\psi_i\}$ forms a complete basis of spinors, we can expand the Elko field as

$$\eta(x) = \sum_i \chi_i \psi_i(x), \quad \bar{\eta}(x) = \sum_i \bar{\chi}_i \psi_i^\dagger(x), \quad (14)$$

where χ_i and $\bar{\chi}_i$ are independent Grassmann variables. Therefore, $V_E^{(1)}$ becomes

$$V_E^{(1)} = -\frac{1}{\Omega_4} \ln \int \prod_j \frac{d\bar{\chi}_j d\chi_j}{\alpha^2} \exp \left(-\sum_j \bar{\chi}_j \chi_j \Lambda_j \right), \quad (15)$$

where the mass-dimensional constant α is an integration measure in the functional space of the Elko field. Expanding the exponential and using the properties of Grassmann integrals, one finds

$$V_E^{(1)} = -\frac{1}{\Omega_4} \ln \prod_j \frac{\Lambda_j}{\alpha^2} = -\frac{1}{\Omega_4} \ln \det \frac{\hat{A}}{\alpha^2}. \quad (16)$$

Using the well-known relation between determinants and traces, $\det M = \exp(\text{tr} \ln M)$, we can rewrite this as

$$V_E^{(1)} = -\frac{1}{\Omega_4} \text{tr} \ln \frac{\hat{A}}{\alpha^2} = -\frac{4}{\Omega_4} \sum_i \ln \frac{\Lambda_i}{\alpha^2}, \quad (17)$$

where the factor of 4 comes from the trace of the 4×4 identity matrix.

In Ref. [27], a ϕ -dependent matrix, $\mathcal{G}(\phi)$, is introduced and defined in terms of spin-sum results. It satisfies the property $\mathcal{G}(\phi) = -\mathcal{G}(\phi + \pi)$ and contributes to the system only if a preferred direction exists. In the present setup, however, the contribution of $\mathcal{G}(\phi)$ vanishes due to the axial symmetry around the z -axis and the fact that $\int_0^{2\pi} d\phi \text{tr} \mathcal{G}(\phi) = 0$. Nevertheless, nontrivial effects of $\mathcal{G}(\phi)$ could, in principle, arise in situations where the azimuthal symmetry is explicitly broken. Examples include (i) anisotropic or structured plates that single out a preferred direction in the xy -plane, (ii) the presence of external vector backgrounds that couple differently to distinct azimuthal angles, or (iii) the analysis of directional correlation functions without performing the full angular integration. In such cases, the Fourier zero mode of $\mathcal{G}(\phi)$ would survive and could potentially modify the spectral sums and loop corrections.

Introducing the generalized zeta function [30, 33, 36] constructed from the eigenvalues Λ_j , we can write

$$V_E^{(1)} = \frac{4}{\Omega_4} \left[\zeta'_\eta(0) + \zeta_\eta(0) \ln \alpha^2 \right], \quad (18)$$

where

$$\zeta(s) = \sum_{\sigma} \Lambda_{\sigma}^{-s}, \quad (19)$$

is the generalized zeta function, which converges for $\text{Re}(s) > 2$ and is regular at $s = 0$, admitting an analytic continuation to other values of s . Note that σ represents the set of quantum numbers of the system.

Similarly, for the scalar field we obtain [32–34]:

$$\begin{aligned} V_{\text{R}}^{(1)} &= -\frac{1}{\Omega_4} \ln \int \mathcal{D}\varphi \exp \left(-\frac{1}{2} \int d^4x \varphi \hat{B} \varphi \right) \\ &= -\frac{1}{2\Omega_4} \left[\zeta'_{\varphi}(0) + \zeta_{\varphi}(0) \ln \beta^2 \right]. \end{aligned} \quad (20)$$

Here, β is also a mass-dimensional constant that serves as an integration measure in the functional space of the scalar field. Both α and β are auxiliary parameters that will be removed by imposing appropriate renormalization conditions on the fields.

Collecting the results in Eqs. (18) and (20), the one-loop correction to the effective potential is

$$V^{(1)}(\bar{\Psi}, \Psi, \Phi) = V_{\text{E}}^{(1)}(\bar{\Psi}, \Psi, \Phi) + V_{\text{R}}^{(1)}(\bar{\Psi}, \Psi, \Phi). \quad (21)$$

Comparing Eqs. (18) and (20), one observes that the contribution from the Elko field is eight times larger than that of the real scalar field. This result contrasts with the standard Dirac fermion, whose contribution is four times larger [37]. Furthermore, our finding also differs from that of Ref. [38], where the authors analyzed the partition function associated with the Elko field.

In analogy with the analysis presented in Ref. [27], where the interaction between the Elko field and the Higgs field plays a central phenomenological role, we focus here on the coupling between the Elko field and a real scalar field. This choice is made for the sake of simplicity, allowing a clearer examination of the vacuum energy corrections induced by the scalar-fermionic interaction, while avoiding the additional complications arising from gauge structure or spontaneous symmetry breaking. Nevertheless, the formulation and results presented in this work can be straightforwardly generalized to the case of a complex scalar field-such as the Higgs doublet-since the essential features of the interaction and its impact on the effective potential remain formally analogous.

The two-loop contribution $V^{(2)}(\bar{\Psi}, \Psi, \Phi)$, with the help of Feynman diagrams, can also be expressed in terms of generalized zeta functions if one is only interested in vacuum contributions [31, 32]. Its explicit form will be presented in Sec. IV.

III. GENERALIZED ZETA FUNCTION AND ONE-LOOP CORRECTION

In this section, we employ the generalized zeta-function technique to obtain the one-loop correction to the effective potential of the theory under consideration. The fields satisfy Dirichlet boundary conditions imposed on two large, perfectly reflecting parallel plates separated by a distance L along the z -axis (see Fig. 1).

A. Dirichlet boundary conditions for the Elko and scalar fields

In Ref. [25], the authors analyzed the Casimir energy associated with an Elko field, assuming that the field satisfies Dirichlet boundary conditions on two large plates separated by a distance L . In this section, we revisit this problem by considering a more general situation, in which the Elko field is coupled to a real scalar field. The latter, in turn, is assumed to satisfy the same boundary conditions as the Elko field.

We now want to calculate the one-loop effective potential associated with the Elko field. In the case of Dirichlet boundary conditions, the Elko field η and its conjugate $\bar{\eta}$ satisfy the following relation at the plates [24, 25]:

$$\eta(\tau, x, y, 0) = \eta(\tau, x, y, L) = 0, \quad (22)$$

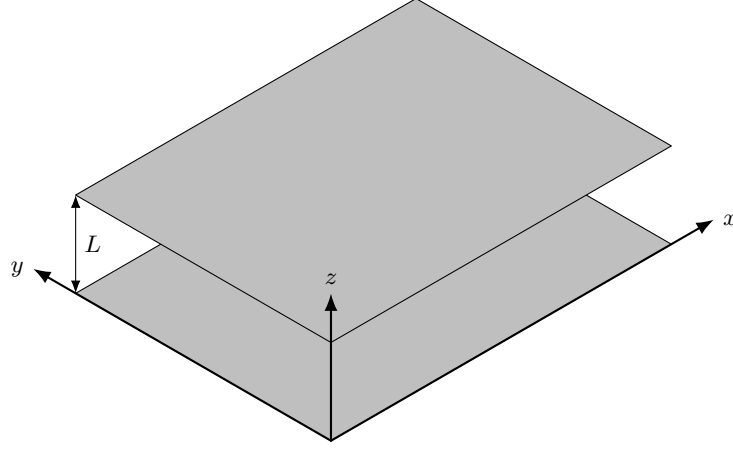


Figure 1. A schematic representation of two perfectly reflecting parallel plates lying in the x - y plane and separated by a distance L along the z -axis is shown. Both the Elko and the real scalar fields satisfy Dirichlet boundary conditions at the plates, located at $z = 0$ and $z = L$.

This plays a crucial role in the evaluation of the effective potential, as it determines the allowed mode spectrum of the field between the boundaries, thereby affecting the summation over quantum fluctuations that contributes to the one-loop corrections.

Therefore, under the above condition, the eigenvalues of the operator \hat{A} , presented in Eq. (11), take the form given by

$$\Lambda_\sigma = k_\tau^2 + k_x^2 + k_y^2 + \left(\frac{n\pi}{L}\right)^2 + M_E^2, \quad n \in \mathbb{Z}_+^*, \quad (23)$$

where the index σ denotes the set of quantum numbers (k_τ, k_x, k_y, n) and we have defined the quantity M_E^2 as

$$M_E^2 = m_E^2 + g\Phi^2. \quad (24)$$

In addition, in the case under consideration, the background field Φ can be taken as non-zero. This will not be the case when dealing with two scalar fields, as in Refs. [33, 34, 39].

The scalar field also obeys Dirichlet boundary conditions, and therefore satisfies a relation analogous to Eq. (22). Hence, the eigenvalues of the operator \hat{B} , Eq. (11), can be written as

$$\Lambda_\sigma = k_\tau^2 + k_x^2 + k_y^2 + \left(\frac{j\pi}{L}\right)^2 + M_g^2, \quad j \in \mathbb{Z}_+^*, \quad (25)$$

where the quantity M_g^2 is defined as

$$M_g^2 = m_R^2 + \frac{\lambda_\varphi}{2}\Phi^2 + 2g\bar{\Psi}\Psi. \quad (26)$$

Here, σ denotes the set of quantum numbers (k_τ, k_x, k_y, j) . Note that in both cases, namely Eqs. (23) and (25), the momenta (k_τ, k_x, k_y) are continuous, whereas j and n are discrete.

B. Loop Correction and Generalized Zeta Functions

Knowing the explicit form of the eigenvalues presented in Eqs. (23) and (25), we can construct the generalized zeta functions associated with each field. We begin by considering the generalized zeta function corresponding to the Elko field. Using the eigenvalues in Eq. (23), the generalized zeta function, Eq. (19), is given by

$$\zeta_E(s) = \frac{\Omega_3}{(2\pi)^3} \int dk_\tau dk_x dk_y \sum_{n=1}^{\infty} \left[k_\tau^2 + k_y^2 + k_x^2 + \left(\frac{n\pi}{L}\right)^2 + M_E^2 \right]^{-s}, \quad (27)$$

where Ω_3 is a volume-like parameter associated with the continuous momenta (k_τ, k_x, k_y) .

To rewrite this zeta function in a more convenient form, we follow the procedure outlined, for instance, in [31], highlighting some steps for clarity. First, we use the identity

$$w^{-s} = \frac{2}{\Gamma(s)} \int_0^\infty d\rho \rho^{2s-1} e^{-w\rho^2}, \quad (28)$$

and perform the resulting Gaussian integrals. This yields an expression suitable for identifying the integral representation of the gamma function $\Gamma(z)$ [40], namely

$$\frac{\Gamma(s)}{2} = \int_0^\infty d\mu \mu^{2s-1} e^{-\mu^2}. \quad (29)$$

Following these steps, the generalized zeta function associated with the Elko field can be expressed as

$$\zeta_E(s) = \frac{\Omega_4 \pi^{\frac{3}{2}-2s}}{8L^{4-2s}} \frac{\Gamma(s-\frac{3}{2})}{\Gamma(s)} \sum_{n=1}^{\infty} \left(n^2 + \frac{M_E^2 L^2}{\pi^2} \right)^{\frac{3}{2}-s}, \quad (30)$$

where $\Omega_4 = \Omega_3 L$. Using the Epstein-Hurwitz zeta function [41, 42], i.e.,

$$\begin{aligned} \sum_{l=1}^{\infty} [l^2 + \kappa^2]^{\frac{3}{2}-s} &= -\frac{\kappa^{3-2s}}{2} + \frac{\sqrt{\pi}}{2} \frac{\Gamma(s-2)}{\Gamma(s-\frac{3}{2})} \kappa^{4-2s} \\ &+ \frac{2\kappa^{2-s} \pi^{s-\frac{3}{2}}}{\Gamma(s-\frac{3}{2})} \sum_{j=1}^{\infty} j^{s-2} K_{s-2}(2\pi j \kappa), \end{aligned} \quad (31)$$

where $K_\gamma(x)$ denotes the Macdonald function [40], we can perform the sum over n in Eq. (30) and rewrite the generalized zeta function as a sum of three terms:

$$\begin{aligned} \zeta_\eta(s) &= -\frac{\Omega_4 M_E^{3-2s}}{16\pi^{\frac{3}{2}} L} \frac{\Gamma(s-\frac{3}{2})}{\Gamma(s)} + \frac{\Omega_4 M_E^{4-2s}}{16\pi^2} \frac{\Gamma(s-2)}{\Gamma(s)} \\ &+ \frac{\Omega_4 M_E^{2-s}}{4\pi^2 L^{2-s}} \frac{1}{\Gamma(s)} \sum_{n=1}^{\infty} n^{s-2} K_{s-2}(2n M_E L). \end{aligned} \quad (32)$$

Evaluating the zeta function and its derivative in the limit $s \rightarrow 0$, we obtain from Eq. (21) the one-loop correction to the effective potential due to the Elko field, i.e.,

$$\begin{aligned} V_E^{(1)}(\bar{\Psi}, \Psi, \Phi) &= \frac{M_E^4}{8\pi^2} \left[\frac{3}{2} - \ln \left(\frac{M_E^2}{\alpha^2} \right) \right] - \frac{M_E^3}{3\pi L} \\ &+ \frac{M_E^2}{\pi^2 L^2} \sum_{n=1}^{\infty} n^{-2} K_2(2n M_E L). \end{aligned} \quad (33)$$

Here, the first term on the right-hand side of Eq. (33) is independent of the parameter L and therefore does not contribute to the vacuum energy density. The second term grows with positive powers of the mass and should therefore be discarded. This is consistent with a normalization condition requiring that the renormalized vacuum energy vanish in the large-mass limit [16]. Hence, only the third term contributes to the renormalized vacuum energy density, as we will see later.

By a similar calculation, we construct the generalized zeta function associated with the scalar field. Using the eigenvalues presented in Eq. (25) and following steps analogous to those described above, we obtain

$$\begin{aligned} \zeta_\varphi(s) &= \frac{\Omega_4 M_g^{4-2s}}{16\pi^2} \frac{\Gamma(s-2)}{\Gamma(s)} - \frac{\Omega_4 M_g^{3-2s}}{16\pi^{\frac{3}{2}} L} \frac{\Gamma(s-\frac{3}{2})}{\Gamma(s)} \\ &+ \frac{\Omega_4 M_g^{2-s}}{4\pi^2 L^{2-s}} \frac{1}{\Gamma(s)} \sum_{j=1}^{\infty} j^{s-2} K_{s-2}(2j M_g L). \end{aligned} \quad (34)$$

Evaluating this zeta function and its derivative at $s = 0$, we find the one-loop correction to the effective potential due to the scalar field as

$$\begin{aligned} V_R^{(1)}(\bar{\Psi}, \Psi, \Phi) &= \frac{M_g^4}{64\pi^2} \left[\ln\left(\frac{M_g^2}{\beta^2}\right) - \frac{3}{2} \right] + \frac{M_g^3}{24\pi L} \\ &\quad - \frac{M_g^2}{8\pi^2 L^2} \sum_{j=1}^{\infty} j^{-2} K_2(2jM_g L). \end{aligned} \quad (35)$$

Combining the results from Eqs. (33) and (35), together with Eqs. (7) and (8), we write the non-renormalized effective potential up to one-loop order as

$$\begin{aligned} V_{\text{eff}}(\bar{\Psi}, \Psi, \Phi) &= m_E^2 \bar{\Psi} \Psi + \frac{1}{2} m_R^2 \Phi^2 + \frac{\lambda_\varphi}{4!} \Phi^4 + g \Phi^2 \bar{\Psi} \Psi \\ &\quad + \xi(\bar{\Psi}, \Psi, \Phi, C_i) + \frac{M_E^4}{8\pi^2} \left[\frac{3}{2} - \ln\left(\frac{M_E^2}{\alpha^2}\right) \right] \\ &\quad + \frac{M_g^4}{64\pi^2} \left[\ln\left(\frac{M_g^2}{\beta^2}\right) - \frac{3}{2} \right] + \frac{M_g^3}{24\pi L} - \frac{M_E^3}{3\pi L} \\ &\quad + \frac{M_E^2}{\pi^2 L^2} \sum_{n=1}^{\infty} n^{-2} K_2(2nM_E L) \\ &\quad - \frac{M_g^2}{8\pi^2 L^2} \sum_{j=1}^{\infty} j^{-2} K_2(2jM_g L). \end{aligned} \quad (36)$$

Note that although the effective potential above may in principle exhibit several minima, we restrict ourselves to the vacuum defined at

$$v = (\bar{\Psi}, \Psi, \Phi) = (0, 0, 0). \quad (37)$$

This choice is motivated by the fact that it preserves the symmetries of the theory, corresponds to the trivial background around which the perturbative expansion is consistently performed, and provides a natural renormalization point where the physical parameters (masses and couplings) are defined.

Before proceeding to the calculation of the vacuum energy, it is necessary to renormalize the effective potential in Eq. (36). The renormalization conditions, taken at the vacuum state v , are given by

$$\left. \frac{d^4 V_{\text{eff}}}{d\Phi^4} \right|_v = \lambda_\varphi, \quad \left. \frac{d^4 V_{\text{eff}}}{d\Phi^2 d\Psi d\bar{\Psi}} \right|_v = 2g, \quad (38)$$

for the self- and cross-couplings, respectively. These conditions determine the renormalization constants C_1 and C_5 , according to Eqs. (8) and (9).

In addition, to determine the coefficients C_2 and C_4 one must impose renormalization conditions for the masses of the real scalar and Elko fields, respectively, as follows:

$$\left. \frac{d^2 V_{\text{eff}}}{d\Phi^2} \right|_v = m_R^2, \quad \left. \frac{d^2 V_{\text{eff}}}{d\Psi d\bar{\Psi}} \right|_v = m_E^2. \quad (39)$$

A final condition is still required to determine the coefficient C_3 . This is done by imposing that the effective potential vanishes in the vacuum state v , i.e.,

$$V_{\text{eff}}|_v = 0. \quad (40)$$

Note that the conditions above follow in accordance with Refs. [32–34]. It is worth noticing that the second condition in Eq. (38) for g arises as a consequence of the background field Φ being nonzero, in contrast to Refs. [32–34]. Moreover, these conditions are to be applied in the Minkowski spacetime limit, $L \rightarrow \infty$. Enforcing these conditions determines the explicit form of the renormalization constants C_i in the function $\xi(\bar{\Psi}, \Psi, \Phi, C_i)$ of Eq. (9).

The renormalization procedure is detailed in the Appendix A. Here, we present the renormalization coefficients and the resulting renormalized effective potential. The coefficients are written as

$$\begin{aligned}
C_1 &= \frac{3g^2}{\pi^2} \ln\left(\frac{m_E^2}{\alpha^2}\right) - \frac{3\lambda_\varphi^2}{32\pi^2} \ln\left(\frac{m_R^2}{\beta^2}\right), \\
C_2 &= \frac{\lambda_\varphi m_R^2}{32\pi^2} \left[1 - \ln\left(\frac{m_R^2}{\beta^2}\right)\right] + \frac{gm_E^2}{2\pi^2} \left[\ln\left(\frac{m_E^2}{\alpha^2}\right) - 1\right], \\
C_3 &= -\frac{m_E^4}{8\pi^2} \left[\frac{3}{2} - \ln\left(\frac{m_E^2}{\alpha^2}\right)\right] - \frac{m_R^4}{64\pi^2} \left[\ln\left(\frac{m_R^2}{\beta^2}\right) - \frac{3}{2}\right], \\
C_4 &= -\frac{gm_R^2}{32\pi^2} - \frac{4m_R^2 g}{54\pi^2} \left[\ln\left(\frac{m_R^2}{\beta^2}\right) - \frac{3}{2}\right], \\
C_5 &= -\frac{g\lambda_\varphi}{32\pi^2} \left[\ln\left(\frac{m_R^2}{\beta^2}\right) - \frac{3}{2}\right].
\end{aligned} \tag{41}$$

These coefficients yield the renormalized effective potential as follows:

$$\begin{aligned}
V_{\text{eff}}^{\text{ren}}(\bar{\Psi}, \Psi, \Phi) &= m_E^2 \bar{\Psi} \Psi + \frac{1}{2} m_R^2 \Phi^2 + \frac{\lambda_\varphi}{4!} \Phi^4 + g \Phi^2 \bar{\Psi} \Psi \\
&\quad + \frac{g^2 \Phi^4}{8\pi^2} \left[\frac{3}{2} - \ln\left(\frac{M_E^2}{m_E^2}\right)\right] + \frac{\lambda_\varphi^2 \Phi^4}{256\pi^2} \left[\ln\left(\frac{M_g^2}{m_R^2}\right) - \frac{3}{2}\right] \\
&\quad + \frac{gm_E^2 \Phi^2}{4\pi^2} \left[\frac{1}{2} - \ln\left(\frac{M_E^2}{m_E^2}\right)\right] + \frac{\lambda_\varphi m_R^2 \Phi^2}{64\pi^2} \left[\ln\left(\frac{M_g^2}{m_R^2}\right) - \frac{1}{2}\right] \\
&\quad - \frac{m_E^4}{8\pi^2} \ln\left(\frac{M_E^2}{m_E^2}\right) + \frac{m_R^4}{64\pi^2} \ln\left(\frac{m_R^2 + \frac{\lambda_\varphi}{2} \Phi^2}{m_R^2}\right) \\
&\quad + \frac{m_R^4 g \bar{\Psi} \Psi}{32\pi^2 \left(m_R^2 + \frac{\lambda_\varphi}{2} \Phi^2\right)} + \frac{g \lambda_\varphi \Phi^2 \bar{\Psi} \Psi}{32\pi^2} \ln\left(\frac{m_R^2 + \frac{\lambda_\varphi}{2} \Phi^2}{m_R^2}\right) \\
&\quad + \frac{gm_R^2 \bar{\Psi} \Psi}{16\pi^2} \left[\ln\left(\frac{m_R^2 + \frac{\lambda_\varphi}{2} \Phi^2}{m_R^2}\right) - \frac{1}{2}\right] \\
&\quad + \frac{M_E^2}{\pi^2 L^2} \sum_{n=1}^{\infty} n^{-2} K_2(2nM_E L) - \frac{M_g^2}{8\pi^2 L^2} \sum_{j=1}^{\infty} j^{-2} K_2(2jM_g L).
\end{aligned} \tag{42}$$

Having established the explicit form of the renormalized effective potential for the system of an Elko field interacting with a real scalar field, we can now proceed to analyze the vacuum energy, its quantum corrections, and the topological mass of the theory.

IV. VACUUM ENERGY PER UNIT AREA OF THE PLATES, FIRST-ORDER COUPLING-CONSTANT CORRECTIONS, AND TOPOLOGICAL MASS

Knowing the explicit form of the renormalized effective potential presented in Eq. (42), we calculate the vacuum energy per unit area, A , of the plates by evaluating it at the vacuum state given in Eq. (37). Therefore, we have

$$\begin{aligned}
\frac{E}{A} &= L V_{\text{eff}}^{\text{ren}}(v) \\
&= \frac{m_E^2}{\pi^2 L} \sum_{n=1}^{\infty} n^{-2} K_2(2nm_E L) - \frac{m_R^2}{8\pi^2 L} \sum_{j=1}^{\infty} j^{-2} K_2(2jm_R L).
\end{aligned} \tag{43}$$

The first term on the r.h.s. of Eq. (43) corresponds to the Elko field satisfying Dirichlet boundary conditions, while the second term represents the contribution from the real scalar field, in agreement with previous results

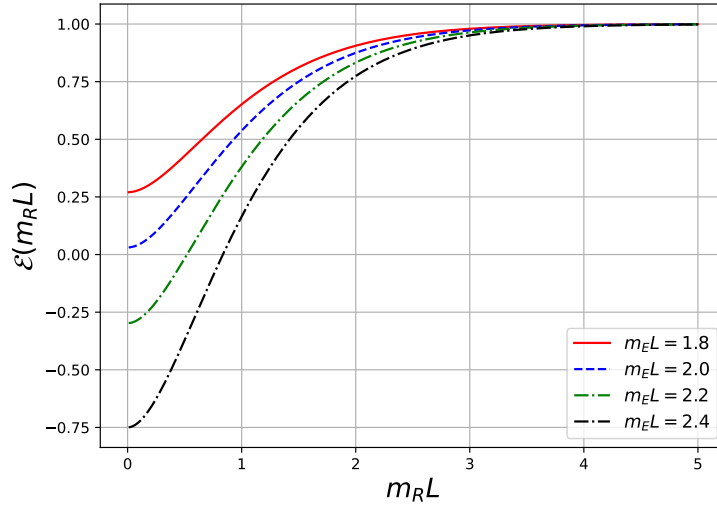


Figure 2. Graph of the dimensionless energy $\mathcal{E}(m_R L)$, Eq. (44), as a function of $m_R L$ and fixed values of $m_E L$.

found in the literature [31, 43]. Note that the Elko term is positive, reflecting its fermionic nature. In contrast with the results found in Refs. [24, 25], the Elko contribution in Eq. (43) is four times larger. This result is further confirmed using canonical quantization, as shown in Appendix B.

In Figure 2 we exhibit the behavior of dimensionless energy $\mathcal{E}(m_R L)$, as a function of $m_R L$, defined as

$$\mathcal{E}(m_R L) = \frac{EL^3\pi^2}{A\varepsilon_E} = 1 - \frac{L^2m_R^2}{8\varepsilon_E} \sum_{j=1}^{\infty} j^{-2} K_2(2jm_R L), \quad (44)$$

where

$$\varepsilon_E = \frac{1}{L^2m_E^2} \sum_{n=1}^{\infty} n^{-2} K_2(2nm_E L). \quad (45)$$

The graph shows that in the limit of large $m_R L$ the dimensionless energy goes to unity, that is, the contribution in this case comes only from the Elko field, as it should be. In addition, increasing the value of $m_E L$ we see that the vacuum energy decreases.

We may also, in principle, consider the massless limit only for the real scalar field. The fundamental anticommutation relations involving the Elko field operators depend on the inverse mass and are therefore ill-defined in the massless limit. This behavior is a consequence of the nonlocal nature of the Elko field (see Ref. [27]). An additional noteworthy feature of this field is that it becomes local as its mass increases.

The massless limit of the real field has been investigated in several other works, for instance in Refs. [16, 31]. This limit can be obtained by considering, in Eq. (43),

$$\lim_{z \rightarrow 0} z^\nu K_\nu(z) = 2^{\nu-1} \Gamma(\nu), \quad (46)$$

for the Macdonald function $K_\nu(z)$, along with the known value of the Riemann zeta function $\zeta(4) = \frac{\pi^4}{90}$ [41, 44].

A. First-Order Coupling-Constant Corrections to the Vacuum Energy

Using the generalized zeta function and Feynman diagrams, one can compute the two-loop correction to the vacuum energy per unit area of the plates in Eq. (43), evaluated at the vacuum state v . The procedure is

described in Refs. [32–34, 39, 45]. The diagrams corresponding to the self-interaction and cross-interaction contributions are shown below:

$$V^{(2)}(v) = \text{---} + \text{---} \quad (47)$$

The contribution from the real scalar field, due to the self-interaction term $\frac{\lambda_\varphi}{4!}\varphi^4$, can be obtained from the first diagram on the r.h.s. of Eq. (47). Mathematically, this translates into

$$\begin{aligned} V_{\lambda_\varphi}^{(2)}(0) &= \frac{3\lambda_\varphi}{4!} \left[\frac{\zeta_\varphi^{\text{ren}}(1)}{\Omega_4} \right]^2 \Big|_v \\ &= \frac{\lambda_\varphi m_R^2}{128\pi^4 L^2} \left[\sum_{n=1}^{\infty} \frac{1}{n} K_1(2nm_R L) \right]^2, \end{aligned} \quad (48)$$

where $\zeta_\varphi^{\text{ren}}(1)$ is the generalized zeta function defined in Eq. (34), with both the divergent part at $s = 1$ (the Minkowski contribution) and the contribution from a single plate subtracted [32, 33, 39, 45], namely,

$$\zeta_\varphi^{\text{ren}}(s) = \zeta_\varphi(s) - \frac{\Omega_4 M_g^{4-2s}}{16\pi^2} \frac{\Gamma(s-2)}{\Gamma(s)} + \frac{\Omega_4 M_g^{3-2s}}{16\pi^{\frac{3}{2}} L} \frac{\Gamma(s-3/2)}{\Gamma(s)}. \quad (49)$$

Note that the factor of three in Eq. (48) originates from the Wick's theorem for field contractions, while the symmetry factor in this case is $\frac{1}{2}$. The corresponding loop implies that the zeta function in Eq. (49) should appear divided by Ω_4 . Moreover, for the diagram under consideration there is a single vertex contributing with a factor $\frac{\lambda_\varphi}{4!}$.

Similarly, the first-order correction arising from the interaction between the fields is proportional to the coupling constant g , i.e.,

$$\begin{aligned} V_g^{(2)}(0) &= g \left[\frac{\zeta_\eta^{\text{ren}}(1)}{\Omega_4} \frac{\zeta_\varphi^{\text{ren}}(1)}{\Omega_4} \right] \Big|_v \\ &= g \frac{m_E m_R}{16\pi^4 L^2} \left[\sum_{n=1}^{\infty} \frac{1}{n} K_1(2nm_E L) \right] \left[\sum_{j=1}^{\infty} \frac{1}{j} K_1(2jm_R L) \right], \end{aligned} \quad (50)$$

where $\zeta_\eta^{\text{ren}}(1)$ is defined analogously to $\zeta_\varphi^{\text{ren}}(1)$. Note that the diagram representing the mixed terms in Eq. (47) indicates that the corresponding expression involves the product of the coupling constant g (from a single vertex) with the renormalized zeta functions (34) and (32) at $s = 1$, each divided by Ω_4 .

Taking into account the two previous expressions, the total first-order correction to the vacuum energy per unit area of the plates in Eq. (43) is then given by

$$\begin{aligned} \frac{E^{(2)}}{A} &= \frac{\lambda_\varphi m_R^2}{128\pi^4 L} \left[\sum_{n=1}^{\infty} \frac{1}{n} K_1(2nm_R L) \right]^2 \\ &+ \frac{gm_E m_R}{16\pi^4 L} \left[\sum_{n=1}^{\infty} \frac{1}{n} K_1(2nm_E L) \right] \left[\sum_{j=1}^{\infty} \frac{1}{j} K_1(2jm_R L) \right]. \end{aligned} \quad (51)$$

Once again, the massless limit of the Elko field is not well-defined, whereas in the case of the real field it can be obtained by applying the limit given in Eq. (46).

From this point onward, we shall consider the mass corrections to the fields, which arise from the boundary conditions and the interactions in the theory. The topological mass is computed from the renormalization conditions in Eq. (39); however, we must take into account the renormalized effective potential. We first analyze the topological mass associated with the Elko field, and then the mass correction corresponding to the Higgs field.

B. Topological mass of the Elko field

We first consider the mass correction to the Elko field. For this purpose, we have to compute two derivatives of the renormalized effective potential at the vacuum state, Eq. (39), namely,

$$m_T^2 = \left. \frac{d^2 V_{\text{eff}}^{\text{ren}}}{d\Psi d\bar{\Psi}} \right|_v. \quad (52)$$

In the effective potential given in Eq. (42), the first term in the last line does not depend on $\bar{\Psi}$ or Ψ . Therefore, we focus on the second term, since all the other terms vanish once the vacuum state is taken. Because $\bar{\Psi}$ and Ψ are Grassmann variables, the derivatives cannot be taken directly. First, we expand the term M_g in the argument of the Macdonald function $K_\gamma(z)$ in Eq. (42) with respect to $\Psi\bar{\Psi}$ up to first order, using the properties of Grassmann variables. This yields

$$M_g = \left(m_H^2 + \frac{\lambda_\varphi}{2} \Phi^2 + 2g \bar{\Psi} \Psi \right)^{\frac{1}{2}} = M_\Phi + \frac{g \bar{\Psi} \Psi}{M_\Phi}, \quad (53)$$

where we have defined the quantity M_Φ as

$$M_\Phi = \left(m_H^2 + \frac{\lambda_\varphi}{2} \Phi^2 \right)^{\frac{1}{2}}. \quad (54)$$

Note that, due to the Grassmann nature of the variables $\Psi\bar{\Psi}$, which are proportional to a single Grassmann variable, all higher-order terms in Eq. (53) vanish.

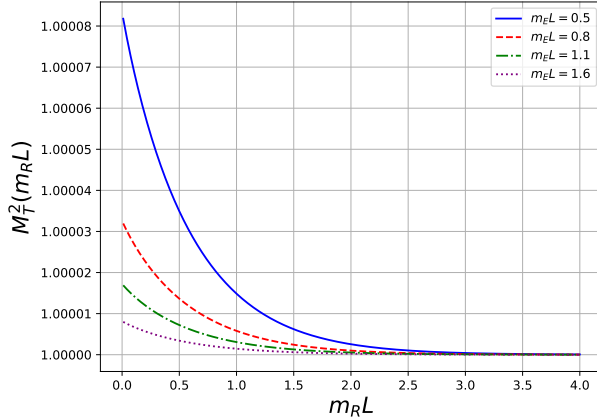


Figure 3. Graph of $M_T^2(m_R L)$, Eq. (59), as a function of $m_R L$, with $g = 10^{-3}$.

The next step is to use the following integral representation of the Macdonald function [46]:

$$K_\alpha(x) = \int_0^\infty dt \cosh(\alpha t) e^{-x \cosh t}, \quad (55)$$

which leads to

$$K_2(jM_g L) = \int_0^\infty dt \cosh(2t) \exp \left[-jL \left(M_\Phi + \frac{g \bar{\Psi} \Psi}{M_\Phi} \right) \cosh t \right]. \quad (56)$$

Expanding the exponential in the above equation and using the properties of the Grassmann variables, we obtain the Macdonald function in the following form:

$$K_2(jM_g L) = K_2(jM_\Phi L) + jgL \frac{\bar{\Psi} \Psi}{M_\Phi} \frac{dK_2(jM_\Phi L)}{d(jM_\Phi L)}. \quad (57)$$

In this form, it is straightforward to take the derivatives. Therefore, we obtain the topological mass of the Elko field as

$$m_T^2 = m_E^2 + \frac{g m_R}{4\pi^2 L} \sum_{j=1}^{\infty} j^{-1} K_1(2j m_R L). \quad (58)$$

Note that the field acquires a mass correction proportional to the coupling constant g and exhibits a dependence on the distance L (related to the boundary conditions) as well as on the mass of the scalar field m_R .

In Figure 3 we exhibit the behavior of dimensionless topological mass squared associated with the Elko field,

$$M_T^2(m_R L) = \frac{m_T^2}{m_E^2} = 1 + \frac{g m_R L}{4\pi^2 m_E^2 L^2} \sum_{j=1}^{\infty} j^{-1} K_1(2j m_R L), \quad (59)$$

as a function of $m_R L$, with fixed value $g = 10^{-3}$ and $m_E L = 0.5, 0.8, 1.1, 1.6$. As already mentioned, the massless limit of the above expression can be taken only for the real scalar field, using Eq. (46).

Next, we consider the topological mass associated with the real scalar field.

C. Topological Mass of the Real Scalar Field

Considering the real scalar field, the derivatives of the renormalized effective potential is expressed as

$$m_T^2 = \left. \frac{d^2 V_{\text{eff}}^{\text{ren}}}{d\Phi^2} \right|_v.$$

This provides the following expression for the topological mass of the real scalar field

$$\begin{aligned} m_T^2 = m_R^2 - \frac{2g m_E}{\pi^2 L} \sum_{n=1}^{\infty} n^{-1} K_1(2n m_E L) \\ + \frac{\lambda_\varphi m_R}{8\pi^2 L} \sum_{j=1}^{\infty} j^{-1} K_1(2j m_R L). \end{aligned} \quad (60)$$

Note that one term of the correction is proportional to the coupling constant g , since it comes from the

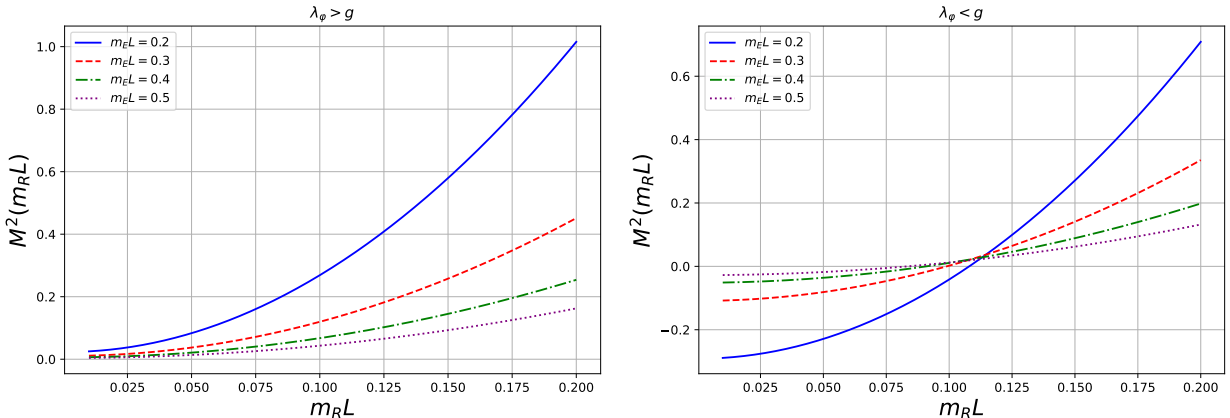


Figure 4. The graph on the left shows the $M^2(m_R L)$, Eq. (61), with $g = 10^{-3}$ and $\lambda_\varphi = 10^{-1}$, as a function of $m_R L$, while the graph on the right takes the values $g = 10^{-1}$ and $\lambda_\varphi = 10^{-3}$.

interaction between the fields and it also depends on the mass of the Elko field. The other correction comes

from the self-interaction of the real scalar field, so it is proportional to the coupling constant λ_φ . Moreover, the two terms also depends on the parameter L related with the boundary condition.

Figure 4 shows the graph of the dimensionless topological mass associated with the real field,

$$\begin{aligned} M^2(m_R L) = & \frac{m_T^2}{m_E^2} = \frac{m_E^2 L^2}{m_E^2 L^2} - \frac{2g}{\pi^2 m_E L} \sum_{n=1}^{\infty} n^{-1} K_1(2n m_E L) \\ & + \frac{\lambda_\varphi m_R L}{8\pi^2 m_E^2 L^2} \sum_{j=1}^{\infty} j^{-1} K_1(2j m_R L), \end{aligned} \quad (61)$$

as a function of $m_R L$ and fixed values $m_E L = 0.2, 0.3, 0.4, 0.5$. The graph on the left takes the values $g = 10^{-3}$ and $\lambda_\varphi = 10^{-1}$. As we can see, the graph on the left is strictly positive, since $\lambda_\varphi > g$. However, the graph on the right shows possibilities for negative values of the squared mass, which in principle indicates vacuum instability [33].

V. CONCLUDING REMARKS

In this work, we have analyzed the quantum vacuum properties of a four-dimensional system composed of a mass-dimension-one fermionic field (Elko) interacting with a real scalar field through a quadratic coupling, both subjected to Dirichlet boundary conditions on two parallel plates separated by a distance L . Using the path integral formalism and the effective potential method, we evaluated the renormalized vacuum energy density, including first-order corrections due to the interaction term, and derived the corresponding topological mass corrections for each field.

Our results show that the presence of boundaries and interactions produce nontrivial modifications to the vacuum structure of the theory. In particular, the contribution of the Elko field to the vacuum energy is significantly enhanced compared to that of the scalar field, while the first-order coupling corrections generate boundary-induced mass shifts that depend explicitly on the plate separation. These topological mass corrections encode the interplay between quantum fluctuations, geometry, and field interactions, highlighting how non-standard fermionic fields can lead to distinctive signatures in confined geometries.

In addition to the analytical results, we exhibit numerically the dependence of the vacuum energy associated with the scalar and Elko fields as function of $m_R L$ in Fig. 2. Also we present in Figs. 3 and 4, the behavior of the topological mass associated with the Elko and scalar fields, respectively. In all these graphs, we observe that they go to zero in the limit of large value for L .

Moreover, the analysis indicates that, depending on the parameter regime, the scalar sector may develop negative topological mass corrections, signaling potential boundary-induced instabilities or spontaneous symmetry breaking. Such effects could point to the existence of multiple vacua or metastable configurations, a feature that merits further investigation through a detailed vacuum stability analysis.

Although our study focused on a real scalar field for simplicity, the formalism can be directly extended to complex scalar fields, including the Higgs doublet, preserving the essential features of the Elko - scalar interaction. Future work may explore higher-loop corrections, finite-temperature effects, or curved-space generalizations, aiming to connect these boundary-induced quantum phenomena with broader aspects of Elko phenomenology and dark matter models.

ACKNOWLEDGMENTS

The authors are grateful to Prof. D. Grumiller and Prof. Andrea Erdas for useful discussions. H.F.S.M. is partially supported by the Brazilian agency National Council for Scientific and Technological Development (CNPq) under Grant No. 308049/2023-3. The author E.R.B.M. thanks CNPq for partial support, Grant No. 304332/2024-0.

Appendix A: On renormalization

In this section, we apply the renormalization conditions presented in Eq. (38). These conditions are imposed on the effective potential, Eq. (36), in the Minkowski spacetime limit, that is, $L \rightarrow \infty$. In addition,

terms proportional to the third power of the masses are neglected, as is customary when considering Dirichlet boundary conditions [31]. Therefore, the part of the effective potential relevant for the renormalization procedure reads

$$\begin{aligned} V_{\text{eff}} = & m_E^2 \bar{\Psi} \Psi + \frac{1}{2} m_H^2 \Phi^2 + \frac{\lambda_\varphi}{4!} \Phi^4 + g \Phi^2 \bar{\Psi} \Psi \\ & + \frac{C_1}{4!} \Phi^4 + \frac{C_2}{2} \Phi^2 + C_3 + C_4 \bar{\Psi} \Psi + C_5 \Phi^2 \bar{\Psi} \Psi \\ & + \frac{M_E^4}{2^3 \pi^2} \left(\frac{3}{2} - \ln \frac{M_E^2}{\alpha^2} \right) + \frac{M_g^4}{2^6 \pi^2} \left(\ln \frac{M_g^2}{\beta^2} - \frac{3}{2} \right). \end{aligned} \quad (\text{A1})$$

We first apply the renormalization conditions associated with the scalar field. The first condition in Eq. (38) gives

$$C_1 = \frac{3}{\pi^2} g^2 \ln \frac{m_E^2}{\alpha^2} - \frac{3\lambda_\varphi^2}{2^5 \pi^2} \ln \frac{m_H^2}{\beta^2}. \quad (\text{A2})$$

The renormalization condition (39) associated with the scalar field determines the constant C_2 as

$$C_2 = \frac{\lambda_\varphi m_H^2}{2^5 \pi^2} \left(1 - \ln \frac{m_H^2}{\beta^2} \right) + \frac{g m_E^2}{2 \pi^2} \left(\ln \frac{m_E^2}{\alpha^2} - 1 \right). \quad (\text{A3})$$

Next, applying the third condition in Eq. (40), we obtain the constant C_3 as

$$C_3 = -\frac{m_E^4}{2^3 \pi^2} \left(\frac{3}{2} - \ln \frac{m_E^2}{\alpha^2} \right) - \frac{m_H^4}{2^6 \pi^2} \left(\ln \frac{m_H^2}{\beta^2} - \frac{3}{2} \right). \quad (\text{A4})$$

After substituting the renormalization constants (A2)-(A4) into Eq. (A1), the renormalized effective potential becomes

$$\begin{aligned} V_{\text{eff}} = & m_E^2 \bar{\Psi} \Psi + \frac{1}{2} m_H^2 \Phi^2 + \frac{\lambda_\varphi}{4!} \Phi^4 + g \Phi^2 \bar{\Psi} \Psi + \xi(\bar{\Psi}, \Psi, C_i) \\ & + \frac{g^2 \Phi^4}{2^3 \pi^2} \left[\frac{3}{2} - \ln \left(\frac{M_E^2}{m_E^2} \right) \right] + \frac{\lambda_\varphi^2 \Phi^4}{2^8 \pi^2} \left[\ln \left(\frac{M_g^2}{m_H^2} \right) - \frac{3}{2} \right] \\ & + \frac{g m_E^2 \Phi^2}{2^2 \pi^2} \left[\frac{1}{2} - \ln \left(\frac{M_E^2}{m_E^2} \right) \right] + \frac{\lambda_\varphi m_H^2 \Phi^2}{2^6 \pi^2} \left[\ln \left(\frac{M_g^2}{m_H^2} \right) - \frac{1}{2} \right] \\ & - \frac{m_E^4}{2^3 \pi^2} \ln \left(\frac{M_E^2}{m_E^2} \right) + \frac{m_H^4}{2^6 \pi^2} \ln \left(\frac{M_g^2}{m_H^2} \right) \\ & + \frac{(4m_H^2 g \bar{\Psi} \Psi + 2\lambda_\varphi g \Phi^2 \bar{\Psi} \Psi)}{2^6 \pi^2} \left[\ln \left(\frac{M_g^2}{\beta^2} \right) - \frac{3}{2} \right], \end{aligned} \quad (\text{A5})$$

where we take $(\bar{\Psi} \Psi)^2 = 0$, since it is proportional to a single Grassmann variable, and

$$\xi(\bar{\Psi}, \Psi, C_i) = C_4 \bar{\Psi} \Psi + C_5 \Phi^2 \bar{\Psi} \Psi. \quad (\text{A6})$$

Now we take the renormalization conditions associated with the Elko field. First, we rewrite the logarithmic function as

$$\ln \left(\frac{M_g^2}{\beta^2} \right) = \ln \left(\frac{m_H^2 + \frac{\lambda_\varphi}{2} \Phi^2}{\beta^2} \right) + \ln \left(1 + \frac{2g \bar{\Psi} \Psi}{m_H^2 + \frac{\lambda_\varphi}{2} \Phi^2} \right), \quad (\text{A7})$$

and, using the expansion

$$\ln(1 + x) = \sum_{n=1}^{\infty} (-1)^{n+1} \frac{x^n}{n}, \quad (\text{A8})$$

together with the fermionic property of the Elko field, we find

$$\ln \left(\frac{M_g^2}{\beta^2} \right) = \ln \left(\frac{m_H^2 + \frac{\lambda_\varphi}{2} \Phi^2}{\beta^2} \right) + \frac{2g\bar{\Psi}\Psi}{m_H^2 + \frac{\lambda_\varphi}{2} \Phi^2}. \quad (\text{A9})$$

We can now apply the condition associated with the mass of the Elko field, that is, the second condition in Eq. (39), which gives the fourth renormalization constant as

$$C_4 = -\frac{gm_H^2}{2^5\pi^2} - \frac{4m_H^2g}{2^6\pi^2} \left(\ln \frac{m_H^2}{\beta^2} - \frac{3}{2} \right). \quad (\text{A10})$$

Applying the second condition in Eq. (38), we obtain the last renormalization constant:

$$C_5 = -\frac{g\lambda_\varphi}{2^5\pi^2} \left(\ln \frac{m_H^2}{\beta^2} - \frac{3}{2} \right). \quad (\text{A11})$$

Substituting the renormalization constants obtained in Eqs. (A10) and (A11) into the potential of Eq. (A5), and adding the terms that depend on L , we obtain the renormalized effective potential associated with the system studied here, that is,

$$\begin{aligned} V_{\text{eff}}^{\text{ren}}(\bar{\Psi}, \Psi, \Phi) = & m_E^2 \bar{\Psi}\Psi + \frac{1}{2} m_H^2 \Phi^2 + \frac{\lambda_\varphi}{4!} \Phi^4 + g\Phi^2 \bar{\Psi}\Psi \\ & + \frac{g^2\Phi^4}{2^3\pi^2} \left[\frac{3}{2} - \ln \left(\frac{M_E^2}{m_E^2} \right) \right] + \frac{\lambda_\varphi^2\Phi^4}{2^8\pi^2} \left[\ln \left(\frac{M_g^2}{m_H^2} \right) - \frac{3}{2} \right] \\ & + \frac{gm_E^2\Phi^2}{2^2\pi^2} \left[\frac{1}{2} - \ln \left(\frac{M_E^2}{m_E^2} \right) \right] + \frac{\lambda_\varphi m_H^2\Phi^2}{2^6\pi^2} \left[\ln \left(\frac{M_g^2}{m_H^2} \right) - \frac{1}{2} \right] \\ & - \frac{m_E^4}{2^3\pi^2} \ln \left(\frac{M_E^2}{m_E^2} \right) + \frac{m_H^4}{2^6\pi^2} \ln \left(\frac{m_H^2 + \frac{\lambda_\varphi}{2}\Phi^2}{m_H^2} \right) \\ & + \frac{m_H^4 g \bar{\Psi}\Psi}{2^5\pi^2 \left(m_H^2 + \frac{\lambda_\varphi}{2}\Phi^2 \right)} + \frac{g\lambda_\varphi \Phi^2 \bar{\Psi}\Psi}{2^5\pi^2} \ln \left(\frac{m_H^2 + \frac{\lambda_\varphi}{2}\Phi^2}{m_H^2} \right) \\ & + \frac{gm_H^2 \bar{\Psi}\Psi}{2^4\pi^2} \left[\ln \left(\frac{m_H^2 + \frac{\lambda_\varphi}{2}\Phi^2}{m_H^2} \right) - \frac{1}{2} \right] \\ & + \frac{M_E^2}{\pi^2 L^2} \sum_{n=1}^{\infty} n^{-2} K_2(2nM_E L) - \frac{M_g^2}{2^3\pi^2 L^2} \sum_{j=1}^{\infty} j^{-2} K_2(2jM_g L). \end{aligned} \quad (\text{A12})$$

Appendix B: Canonical quantization

In this appendix we compute the vacuum energy using the energy-momentum tensor. The field expansion for the Elko field reads [24]

$$\begin{aligned} \hat{\eta}(x) &= \int \frac{d^3p}{(2\pi)^{3/2} \sqrt{2mE}} \sum_{\alpha} \left[\hat{a}_{\alpha}(\mathbf{p}) \lambda_{\alpha}^S(\mathbf{p}) e^{-ip_{\mu}x^{\mu}} + \hat{a}_{\alpha}^{\dagger}(\mathbf{p}) \lambda_{\alpha}^A(\mathbf{p}) e^{ip_{\mu}x^{\mu}} \right], \\ \hat{\bar{\eta}}(x) &= \int \frac{d^3p}{(2\pi)^{3/2} \sqrt{2mE}} \sum_{\alpha'} \left[\hat{a}_{\alpha'}^{\dagger}(\mathbf{p}) \bar{\lambda}_{\alpha'}^S(\mathbf{p}) e^{ip_{\mu}x^{\mu}} + \hat{a}_{\alpha'}(\mathbf{p}) \bar{\lambda}_{\alpha'}^A(\mathbf{p}) e^{-ip_{\mu}x^{\mu}} \right]. \end{aligned} \quad (\text{B1})$$

The index α runs over four possibilities, corresponding to the two self-conjugate (S) and two anti-self-conjugate (A) spinors. These obey $\hat{C}\lambda_{\alpha}^{S/A}(\mathbf{p}) = \pm \lambda_{\alpha}^{S/A}(\mathbf{p})$, where \hat{C} is the charge conjugation operator. The creation and annihilation operators satisfy the anticommutation algebra

$$[\hat{a}_{\alpha}(\mathbf{p}), \hat{a}_{\alpha'}^{\dagger}(\mathbf{p}')]_{+} = \delta_{\alpha\alpha'} \delta(\mathbf{p} - \mathbf{p}'), \quad (\text{B2})$$

with all other anticommutators vanishing.

The free Lagrangian for the Elko field is

$$\mathcal{L} = \partial^\mu \bar{\eta} \partial_\mu \eta - m_E^2 \bar{\eta} \eta. \quad (\text{B3})$$

Using this Lagrangian together with Eqs. (B1) and (B2), and the spinor identities [24, 47]

$$\begin{aligned} \bar{\lambda}_{\alpha'}^S(\mathbf{p}) \lambda_\alpha^S(\mathbf{p}) &= 2m_E \delta_{\alpha'\alpha}, \\ \bar{\lambda}_{\alpha'}^A(\mathbf{p}) \lambda_\alpha^A(\mathbf{p}) &= -2m_E \delta_{\alpha'\alpha}, \\ \bar{\lambda}_{\alpha'}^S(\mathbf{p}) \lambda_\alpha^A(\mathbf{p}) &= \bar{\lambda}_{\alpha'}^A(\mathbf{p}) \lambda_\alpha^S(\mathbf{p}) = 0, \end{aligned} \quad (\text{B4})$$

we compute the vacuum energy using

$$E_0 = \int d^3x \langle 0 | T_0^0 | 0 \rangle, \quad (\text{B5})$$

where $|0\rangle$ is the Fock vacuum, $\hat{a}_\alpha(\mathbf{p})|0\rangle = 0$, and T_0^0 is the energy-momentum tensor,

$$T_0^0 = \frac{\partial \mathcal{L}}{\partial(\partial_0 \eta)} \partial_0 \eta + \partial_0 \bar{\eta} \frac{\partial \mathcal{L}}{\partial(\partial_0 \bar{\eta})} - \mathcal{L}. \quad (\text{B6})$$

A direct computation yields

$$\int d^3x T_0^0 = 2 \int d^3p \omega \sum_\alpha [\hat{a}_\alpha^\dagger(\mathbf{p}) \hat{a}_\alpha(\mathbf{p}) - \hat{a}_\alpha(\mathbf{p}) \hat{a}_\alpha^\dagger(\mathbf{p})]. \quad (\text{B7})$$

Using the anticommutation relation (B2) we obtain, under Dirichlet boundary conditions,

$$E_0 = -2 \sum_{n=1}^{\infty} \int d^2p_{\parallel} \omega \sum_\alpha \delta(\mathbf{p}_{\parallel} - \mathbf{p}'_{\parallel}) = -4 \sum_{n=1}^{\infty} \int d^2p_{\parallel} \omega \delta(0), \quad (\text{B8})$$

where the subscript \parallel denotes momenta parallel to the plates, and

$$\omega = \sqrt{\frac{n^2 \pi^2}{L^2} + \mathbf{p}_{\parallel}^2 + m^2}. \quad (\text{B9})$$

The distribution $\delta(0)$ is evaluated using its Fourier representation,

$$\delta(\mathbf{p}_{\parallel} - \mathbf{p}'_{\parallel}) = \frac{1}{(2\pi)^2} \int e^{i\mathbf{r}_{\parallel} \cdot (\mathbf{p}_{\parallel} - \mathbf{p}'_{\parallel})} d^2r_{\parallel}, \quad (\text{B10})$$

yielding, for $\mathbf{p}_{\parallel} = \mathbf{p}'_{\parallel}$,

$$\delta(0) = \frac{A}{(2\pi)^2}, \quad (\text{B11})$$

where A is the area of the plates.

Thus, from Eqs. (B8) and (B11) we obtain

$$E_0 = -\frac{4A}{(2\pi)^2} \sum_{n=1}^{\infty} \int d^2p_{\parallel} \omega. \quad (\text{B12})$$

The overall minus sign is a fermionic feature of the Elko field. The result is eight times bigger than the scalar-field contribution, or twice that of the Dirac field. This contrasts with Refs. [24, 25], where the authors report a factor equal to the Dirac case.

Finally, we emphasize that we neglected the matrix $\mathcal{G}(\phi)$ because our model assumes idealized plates without physical features such as rugosity. Such features break azimuthal symmetry and induce a preferred

direction in the plane of the plates (see Ref. [27]). For ideal plates, the symmetry implies that $\mathcal{G}(\phi)$ yields no contribution.

[1] H. B. Casimir, *On the attraction between two perfectly conducting plates*, in *Proc. Kon. Ned. Akad. Wet.*, vol. 51, p. 793, 1948.

[2] M. J. Sparnaay, *Measurements of attractive forces between flat plates*, *Physica* **24** (1958) 751–764.

[3] G. Bressi, G. Carugno, R. Onofrio and G. Ruoso, *Measurement of the Casimir force between parallel metallic surfaces*, *Phys. Rev. Lett.* **88** (2002) 041804, [[quant-ph/0203002](#)].

[4] S. K. Lamoreaux, *Demonstration of the casimir force in the 0.6 to 6 μ m range*, *Phys. Rev. Lett.* **78** (Jan, 1997) 5–8.

[5] S. Lamoreaux, *Erratum: Demonstration of the casimir force in the 0.6 to 6 μ m range [phys. rev. lett. 78, 5 (1997)]*, *Physical Review Letters* **81** (1998) 5475.

[6] U. Mohideen and A. Roy, *Precision measurement of the Casimir force from 0.1 to 0.9 micrometers*, *Phys. Rev. Lett.* **81** (1998) 4549–4552, [[physics/9805038](#)].

[7] V. M. Mostepanenko, *New experimental results on the casimir effect*, *Brazilian Journal of Physics* **30** (2000) 309–315.

[8] W. J. Kim, M. Brown-Hayes, D. A. R. Dalvit, J. H. Brownell and R. Onofrio, *Anomalies in electrostatic calibrations for the measurement of the casimir force in a sphere-plane geometry*, *Phys. Rev. A* **78** (Aug, 2008) 020101.

[9] Q. Wei, D. A. R. Dalvit, F. C. Lombardo, F. D. Mazzitelli and R. Onofrio, *Results from electrostatic calibrations for measuring the casimir force in the cylinder-plane geometry*, *Phys. Rev. A* **81** (May, 2010) 052115.

[10] M. Bordag, U. Mohideen and V. M. Mostepanenko, *New developments in the casimir effect*, *Physics reports* **353** (2001) 1–205.

[11] V. Mostepanenko, N. Trunov and R. Znajek, *The Casimir Effect and Its Applications*. Oxford science publications. Clarendon Press, 1997.

[12] I. Brevik, K. A. Milton and S. D. Odintsov, *Entropy bounds in r^3 geometries*, *Annals of Physics* **302** (2002) 120–141.

[13] A. Zhang, *Thermal casimir effect in kerr space-time*, *Nuclear Physics B* **898** (2015) 220–228.

[14] C. Henke, *Quantum vacuum energy in general relativity*, *The European Physical Journal C* **78** (2018) 1–4.

[15] K. Milton and I. Brevik, *Casimir physics and applications*, 2019.

[16] M. Bordag, G. L. Klimchitskaya, U. Mohideen and V. M. Mostepanenko, *Advances in the Casimir Effect*, vol. 145 of *International Series of Monographs on Physics*. Oxford University Press, Oxford, 2009.

[17] K. A. Milton, *The Casimir effect: physical manifestations of zero-point energy*. World Scientific, 2001.

[18] A. Romeo and A. A. Saharian, *Casimir effect for scalar fields under Robin boundary conditions on plates*, *J. Phys. A* **35** (2002) 1297–1320, [[hep-th/0007242](#)].

[19] G. Aleixo and H. F. S. Mota, *Thermal Casimir effect for the scalar field in flat spacetime under a helix boundary condition*, *Phys. Rev. D* **104** (2021) 045012, [[2105.08220](#)].

[20] C. A. Escobar, A. Martín-Ruiz, R. Linares and J. M. Silva, *A coherent state approach to the Casimir effect for a massive scalar field in a noncommutative spacetime*, *Annals Phys.* **460** (2024) 169570.

[21] R. Saghian, M. A. Valuyan, A. Seyedzahedi and S. S. Gousheh, *Casimir Energy For a Massive Dirac Field in One Spatial Dimension: A Direct Approach*, *Int. J. Mod. Phys. A* **27** (2012) 1250038, [[1204.3181](#)].

[22] A. Flachi, M. Nitta, S. Takada and R. Yoshii, *Sign flip in the casimir force for interacting fermion systems*, *Physical review letters* **119** (2017) 031601.

[23] A. A. Saharian and E. R. Bezerra de Mello, *Spinor Casimir densities for a spherical shell in the global monopole space-time*, *J. Phys. A* **37** (2004) 3543, [[hep-th/0307261](#)].

[24] S. H. Pereira, J. M. Hoff da Silva and R. dos Santos, *Casimir effect for Elko fields*, *Mod. Phys. Lett. A* **32** (2017) 1730016, [[1611.01013](#)].

[25] R. V. Maluf, D. M. Dantas and C. A. S. Almeida, *The Casimir effect for the scalar and Elko fields in a Lifshitz-like field theory*, *Eur. Phys. J. C* **80** (2020) 442, [[1905.04824](#)].

[26] D. V. Ahluwalia and D. Grumiller, *Dark matter: A Spin one half fermion field with mass dimension one?*, *Phys. Rev. D* **72** (2005) 067701, [[hep-th/0410192](#)].

[27] D. V. Ahluwalia and D. Grumiller, *Spin half fermions with mass dimension one: Theory, phenomenology, and dark matter*, *JCAP* **07** (2005) 012, [[hep-th/0412080](#)].

[28] R. Jackiw, *Functional evaluation of the effective potential*, *Phys. Rev. D* **9** (1974) 1686.

[29] L. H. Ryder, *Quantum field theory*. Cambridge university press, 1996.

[30] D. J. Toms, *Symmetry Breaking and Mass Generation by Space-time Topology*, *Phys. Rev. D* **21** (1980) 2805.

- [31] M. B. Cruz, E. R. Bezerra de Mello and H. F. Santana Mota, *Casimir energy and topological mass for a massive scalar field with Lorentz violation*, *Phys. Rev. D* **102** (2020) 045006, [[2005.09513](#)].
- [32] P. J. Porfirio, H. F. Santana Mota and G. Q. Garcia, *Ground state energy and topological mass in spacetimes with nontrivial topology*, *Int. J. Mod. Phys. D* **30** (2021) 2150056, [[1908.00511](#)].
- [33] A. J. D. F. Junior and H. F. S. Mota, *Casimir effect, loop corrections, and topological mass generation for interacting real and complex scalar fields in minkowski spacetime with different conditions*, *Phys. Rev. D* **107** (Jun, 2023) 125019.
- [34] D. J. Toms, *Interacting Twisted and Untwisted Scalar Fields in a Nonsimply Connected Space-time*, *Annals Phys.* **129** (1980) 334.
- [35] J. Venâncio, L. Filho, H. Mota and A. Mohammadi, *Thermal casimir effect for a dirac field on flat space with a nontrivial circular boundary condition*, *Phys. Rev. D* **110** (Aug, 2024) 045006.
- [36] S. W. Hawking, *Zeta Function Regularization of Path Integrals in Curved Space-Time*, *Commun. Math. Phys.* **55** (1977) 133.
- [37] J. Venâncio, L. Filho, H. Mota and A. Mohammadi, *Thermal casimir effect for a dirac field on flat space with a nontrivial circular boundary condition*, 2024.
- [38] S. H. Pereira and R. S. Costa, *Partition function for a mass dimension one fermionic field and the dark matter halo of galaxies*, *Mod. Phys. Lett. A* **34** (2019) 1950126, [[1807.06944](#)].
- [39] A. J. D. Farias Junior, A. Smirnov, H. F. Santana Mota and E. R. Bezerra de Mello, *Vacuum energy density for interacting real and complex scalar fields in a lorentz symmetry violation scenario*, *International Journal of Modern Physics D* **34** (2025) 2450069, [<https://doi.org/10.1142/S021827182450069X>].
- [40] M. Abramowitz and I. A. Stegun, *Handbook of mathematical functions dover publications*, New York **361** (1965).
- [41] E. Elizalde, *Ten Physical Applications of Spectral Zeta Functions*, vol. 35 of *Lecture Notes in Physics Monographs*. Springer-Verlag, Berlin, Heidelberg, 1995, [10.1007/978-3-540-44757-3](#).
- [42] E. Elizalde, *Explicit analytical continuation of the inhomogeneous epstein zeta function*, Hiroshima University Preprint (Sept., 1994).
- [43] A. J. D. F. Junior, A. Erdas and H. F. Santana Mota, *Vacuum Energy and Topological Mass from a Constant Magnetic Field and Boundary Conditions in Coupled Scalar Field Theories*, [2508.15121](#).
- [44] E. Elizalde, S. D. Odintsov, A. Romeo, A. A. Bytsenko and S. Zerbini, *Zeta regularization techniques with applications*. World Scientific Publishing, Singapore, 1994, [10.1142/2065](#).
- [45] A. J. D. Farias Junior and H. F. Mota Santana, *Loop correction to the scalar Casimir energy density and generation of topological mass due to a helix boundary condition in a scenario with Lorentz violation*, *Int. J. Mod. Phys. D* **31** (2022) 2250126, [[2204.09400](#)].
- [46] I. S. Gradshteyn and I. M. Ryzhik, *Table of integrals, series, and products*. Academic press, 2014.
- [47] D. V. Ahluwalia, *The theory of local mass dimension one fermions of spin one half*, *Advances in Applied Clifford Algebras* **27** (2017) 2247–2285.